B-Myc: N-Terminal Recognition of Myc Binding Proteins†

Robert A. Burton,‡,§ Sampo Mattila,‡,|| Elizabeth J. Taparowsky,⊥ and Carol Beth Post*,‡,⊥,@

Department of Medicinal Chemistry and Molecular Pharmacology, Department of Biological Sciences, Markey Center for Structural Biology, and Purdue Cancer Center, Purdue University, West Lafayette, Indiana 47907

Received February 24, 2006; Revised Manuscript Received April 29, 2006

ABSTRACT: B-Myc is an endogenous, N-terminal homologue of transcription factor c-Myc that lacks the C-terminal DNA binding and protein dimerization domain of c-Myc. Clinical mutations in the c-Myc N-terminal region, and the subsequent misregulation of Myc, are implicated in the development of numerous human cancers. Myc functions to both activate and repress transcription by associating with multiple binding partners. We investigated the structural and dynamical properties of B-Myc, free or associated with the transactivation inhibitor, MM-1, and the activator, TBP, using NMR spectroscopy. B-Myc has no persistent tertiary structure, yet regions corresponding to Myc homology boxes 1 and 2 (MBI and MBII, respectively) have molten globule-like characteristics. B-Myc binds to MM-1 in a specific manner without becoming highly structured. The local regions of B-Myc involved in binding differ for MM-1 and TBP, and regions not identified by mutagenesis are found to be involved in MM-1 binding. The results provide new insights into Myc N-terminal protein−protein interactions. We propose a model for Myc regulation through differential involvement of MBI and MBII in the binding of Myc interacting proteins.

B-Myc is a murine, N-terminal homologue of c-Myc that is 62% identical in sequence (*1*−*4*). Although the physiological role of B-Myc is still under investigation, when coexpressed with c-Myc, B-Myc inhibits transcriptional activation and cellular transformation by c-Myc (*5*). B-Myc expression is regulated by androgens and thus may function in vivo to control cell proliferation in a restricted subset of adult tissues affected by c-Myc (*2*, *4*).

Changes in Myc expression and mutations in Myc are linked directly to the development of cancers that include lymphomas and cancers of the bladder, breast, colon, skin, ovary, and prostate (*6*−*8*). As a contributing factor in tumor development, c-Myc is a key target for therapeutic strategies for controlling this disease (*9*−*11*). In normal cells, Myc proteins regulate many aspects of cellular metabolism and direct the decision of cells to proliferate or to undergo apoptosis (*12*, *13*). The diverse cellular roles of Myc are reflected in the identity of the genes that are regulated by Myc transcription complexes, such as ornithine decarboxylase, cdc25A, p53, and others (*8*, *14*−*17*).

The central members of the mammalian Myc protein family are c-, N-, L-, S-, and B-Myc (*6*, *18*). The cellular functions attributed to Myc proteins are mapped to the structural integrity of highly conserved N- and C-terminal domains (Figure 1A). For all Myc proteins, the N-terminal regions contain two such segments termed Myc homology box I (MBI),[1] residues 45−63 of c-Myc (corresponding B-Myc residues 43−61), and Myc homology box II (MBII), residues 129−141 of c-Myc (corresponding B-Myc residues 119−131) (*6*, *8*). MBI and MBII serve as core motifs through which Myc interacts with a variety of regulatory proteins (*19*). The C-terminal regions of the Myc proteins contain a basic helix−loop−helix leucine zipper (bHLHLZ) motif that mediates the dimerization of Myc with other bHLHLZ proteins (e.g., Mad and Max) and the sequence-specific binding of Myc dimers to DNA (*17*, *20*, *21*). The X-ray crystal structure of the C-terminal region of c-Myc was determined recently to be a heterodimer with Max (*22*), but no atomic-resolution structure of a Myc N-terminal region exists to date.

Many proteins interact with the N-terminal regions of Myc proteins, and the differential binding of these proteins is thought to mediate the function of Myc as a transcriptional activator, transcriptional repressor, inducer of cell proliferation, and initiator of apoptosis (*23*). Here, we examine the interaction of B-Myc with Myc modulator-1 (MM-1) and TATA-binding protein (TBP). MM-1 is a protein that previously has been shown to interact with the N-terminal region of c-Myc (*24*). Using c-Myc truncation mutants in yeast two-hybrid, mammalian two-hybrid, and GST pulldown

† This work was supported by National Institutes of Health (NIH) Grant GM39478 (C.B.P.), a Purdue University reinvestment grant, and the Purdue Cancer Center (CA23568). R.A.B. was supported by a Purdue Research Foundation Fellowship and by NIH Biophysics Training Grant (GM008296).

* To whom correspondence should be addressed: Department of Medicinal Chemistry, Purdue University, 757 Stadium Mall Dr., West Lafayette, IN 47907-2091. Telephone: (765) 494-5980. Fax: (765) 496-1189. E-mail: cbp@purdue.edu.

‡ Department of Medicinal Chemistry and Molecular Pharmacology.

§ Present address: National Institutes of Health, Bethesda, MD 20892.

|| Present address: University of Oulu, Oulu, Finland.

⊥ Department of Biological Sciences and Purdue Cancer Center.

@ Markey Center for Structural Biology.

[1] Abbreviations: MBI, Myc homology box I; MBII, Myc homology box II; MM-1, Myc modulator 1; TBP, TATA-binding protein; NMR, nuclear magnetic resonance.

10.1021/bi060379n CCC: $33.50
Published on Web 07/22/2006

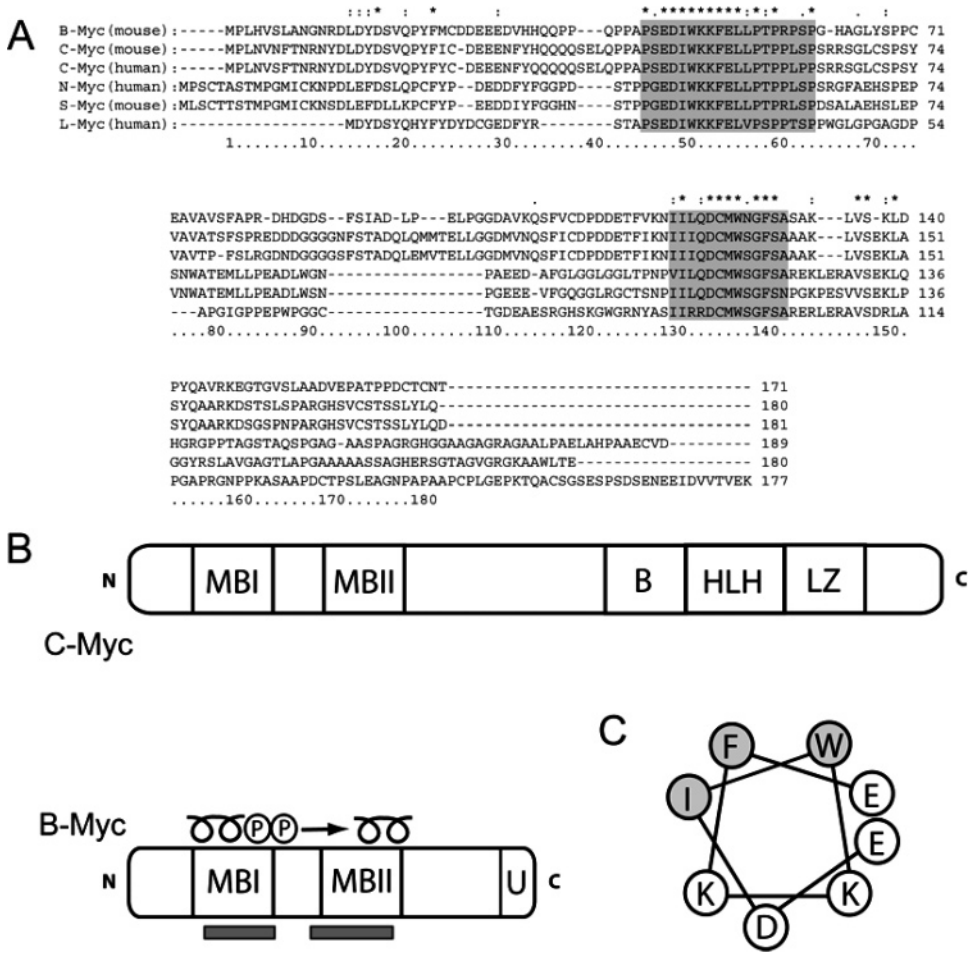

FIGURE 1: (A) Sequence alignment of six Myc family members. Highly conserved regions are indicated above the alignment by asterisks (identical), colons (highly conserved), and periods (conserved). MBI and MBII are highlighted in gray. Panel A was generated with ClustalX (*71*). (B) Schematic diagram of c-Myc and B-Myc with the approximate location of MBI and MBII, the DNA binding region of c-Myc comprising the basic region (B), the helix−loop−helix region (HLH), the leucine zipper (LZ), and the unique region of B-Myc (U). B-Myc secondary structural elements (helix and strand) predicted by PHD are shown above the B-Myc diagram, and ordered regions as predicted by PONDR are shown below. Regulatory phosphorylation sites are also shown. (C) Helical wheel diagram of the predicted amphipathic helix in MBI. Hydrophobic residues are highlighted in gray.

assays, the interaction of MM-1 with c-Myc was mapped to a region spanning MBII (*24*). MM-1 exerts a negative influence on the transactivation of target genes by Myc and inhibits the ability of Myc to transform cells in cooperation with activated Ras (*24*). TBP also interacts with the N-terminal region of c-Myc both in vitro and in vivo but is thought to exert a positive influence on Myc-mediated transactivation (*25*−*28*).

Structural and dynamical information used to define the nature of macromolecular interactions and interfaces was reported for the C-terminal DNA binding and dimerization domain of c-Myc (*22*). For the c-Myc N-terminal region, however, available structural information is limited to a recent NMR structure determination for a complex of a peptide derived from MBI of c-Myc and the SH3 domain of Bin-1 (*29*). In the association of c-Myc with Bin-1, 12 residues of the c-Myc peptide contact Bin-1 and bind in an extended conformation along the surface in the normal poly-Pro site. Structural analysis of the N-terminal domain of Myc has been hampered by the inability to produce sufficient quantities of soluble protein. We have taken advantage of the structural and functional conservation displayed across all members of the Myc family to investigate the structure of the full N-terminal domain using the soluble B-Myc protein, alone and together with transactivation inhibitor MM-1 and the activator TBP using circular dichroism (CD) and NMR spectroscopy. Our data suggest that B-Myc is largely unstructured in solution and that the interaction of B-Myc with MM-1 is mediated not only by MBII, as previously shown, but also by MBI and possibly the unique C-terminal tail. Moreover, the interaction of B-Myc with transcriptional activator TBP was found to be distinct from that of B-Myc with MM-1. These results support a regulatory model in which differential binding of specific residues in the N-terminal regions of Myc proteins leads to either activation or repression of Myc-mediated gene transcription.

MATERIALS AND METHODS

Protein Expression and NMR Sample Preparation. Full-length murine B-Myc (residues 2−169) was expressed in *Escherichia coli* BL21-RP cells (Stratagene) grown in M9 minimal medium as an N-terminal GST-tagged construct in the pGEX-5x-3 vector (Amersham). Nine conservative mutations were introduced into the original construct to replace rare *E. coli* codons. The cell pellet was resuspended in 1XPBS (pH 8.0), 5 mM DTT, protease inhibitor cocktail (Sigma), and 5 mM EDTA and lysed. Clarified lysate was passed over a GSTrap column (Amersham), and the protein

eluted with 1XPBS (pH 8.0) and 20 mM GSH. GST was cleaved using Factor XA (Novagen) and separated from B-Myc using a MonoQ column (Amersham) eluted with a linear NaCl gradient on an ÄktaExplorer-100 instrument (Amersham). Fractions were dialyzed against 20 mM NaH_2PO_4/Na_2HPO_4 (pH 6.0), 100 mM NaCl, and 1 mM DTT and concentrated. Approximately 5−10 mg of B-Myc was obtained per liter of cell culture. The original construct of B-Myc was a gift from M. Gregory (Vanderbilt University, Nashville, TN).

Full-length MM-1 (residues 1−166) was expressed in the pGEX-5x-1 vector in *E. coli* BL21-RP cells in LB. The protocol for B-Myc expression and purification was used for MM-1 except that prior to cleavage with Factor XA, molar equivalent amounts of purified B-Myc were added to maintain the solubility of MM-1. The yield was approximately 30 mg/L of cell culture. The pGEX-5x-1-MM-1 construct was a gift from H. Ariga (Hokkaido University, Hokkaido, Japan).

TATA-binding protein (TBP, residues 1−182) was expressed in the pET-15b vector in *E. coli* BL21-DE3 cells in LB. Pelleted cells were resuspended in 50 mM Tris (pH 8.0), 100 mM KCl, 10% glycerol, and protease inhibitor cocktail and lysed. Clarified lysate was passed over a HiTrap Ni affinity column and eluted with a gradient from 0 to 100 mM imidazole. The eluant fractions were passed over a heparin affinity column (Amersham) and eluted with a gradient from 0 to 1 M NaCl. Fractions containing TBP were dialyzed against 20 mM NaH_2PO_4 (pH 6.0), 100 mM NaCl, and 1 mM DTT and concentrated. The pET-15b-TBP construct was a gift from L. Stargell (Colorado State University, Fort Collins, CO).

NMR experiments were conducted in 5 mm Shigemi tubes in a 90% H_2O/10% D_2O mixture with 20 mM NaH_2PO_4 (pH 6.0), 100 mM NaCl, 5 mM DTT, and 0.01% NaN_3 at final protein concentrations of ∼0.5−1.5 mM as determined by UV_{280} absorption. The B-Myc/MM-1 and B-Myc/TBP samples were prepared at an approximately 1:3 molar ratio.

CD Spectroscopy. CD experiments were conducted using a Jasco J-810 spectropolarimeter at room temperature in 20 mM NaH_2PO_4/Na_2HPO_4 (pH 6.0) and 50 mM NaCl at total protein concentrations of ∼0.5 mg/mL and B-Myc:MM-1 molar ratios 0.5:1, 1:1, and 2:1. Proteins concentrations were determined by UV_{280} absorbance.

NMR Spectroscopy. Triple-resonance experiments were carried out at 300 K on a Varian Inova 800 MHz spectrometer (National Biological NMR Laboratory of Finland) or a Bruker DRX-500 [Purdue Interdepartmental NMR Facility (PINMRF)]. Assignments for main chain and CB resonances of free B-Myc were made by standard methods with data from CT-HNCA, HN(CO)CA, HNCACB, and HN(CO)CACB experiments. For B-Myc in the presence of MM-1 or TBP, the quality of triple-resonance experiments was not adequate for chemical shift assignments.

Relaxation data were measured in duplicate at 300 K with a Bruker DRX-750 MHz spectrometer (National Magnetic Resonance Facility, Madison, WI). T_1 spectra were recorded using delay times of 10, 20, 40, 80, 160, 320, 640, and 1280 ms. T_2 spectra were recorded using delay times of 8, 32, 48, 72, 96, 112, and 128 ms. ^{15}N heteronuclear NOEs were recorded in an interleaved fashion using a 3 ms saturation pulse and an overall delay time of 5 ms (*30*). All spectra were processed with NMRPipe and analyzed using SPARKY version 3.106 (*31*). Only peaks resolved at half-peak height were used in the analysis of the relaxation data. R_1 and R_2 rates were determined using an exponential fit to the signal decay of the selected Lorentzian integrated peak volumes.

RESULTS

Structural Characterization of Free B-Myc. Approximately 86% of the backbone N, H^N, C, C, and CO resonances were assigned for free B-Myc. The amide proton peak dispersion in the ^{15}N HSQC spectrum (Figure 2A) is less than 1 ppm and spans from only 7.7 to 8.6 ppm, similar to the sequence-corrected random coil range of 7.54−8.56 ppm (*32*, *33*). Chemical shift indexing (CSI) showed no consensus for either helical or strand content (data not shown) (*34*). In addition, CD data, discussed below, confirm the absence of secondary structural elements. These results indicate that free B-Myc lacks a stable tertiary fold and does not contain persistent secondary structure.

$^1H-^{15}N$ heteronuclear NOE intensities were measured to further characterize the structure of B-Myc. The data suggest that some degree of structural organization exists for the regions near MBI and MBII despite the lack of overall stable tertiary structure. The NOE value expected for highly mobile HN groups is <0 and for folded proteins the size of B-Myc is >0.7. For a completely unfolded protein with a polymer-like configuration, the NOE value is expected to increase somewhat toward the central region of the chain and fall off near the termini (*35*, *36*). The individual resonance NOE values observed along the B-Myc chain, as well as the trend characterized with a five-residue moving average of the NOE values, are plotted as a function of residue in Figure 3. For the regions surrounding MBI and MBII, the values tend to be relatively larger, while in the center of the protein, between MBI and MBII, the NOE value tends to be smaller and closer to 0 with some residues showing NOE values approaching −0.5 indicating relatively greater mobility. Thus, the pattern is consistent with neither a completely unfolded protein nor a folded protein. The NOE values are 0.1−0.2 for the molten globule form of the H helix from the similarly sized apomyoglobin protein (*37*). Therefore, B-Myc in solution is not a well-ordered globular structure, but the vicinity of MBI and MBII appears to be a more collapsed structure on average, with slower rotational mobility similar to that of molten globule proteins.

In view of the limited structure suggested from the NOE profile, we assessed the level of structure predicted from sequence-based algorithms. Interestingly, both secondary structure (*38*) and ordered structure (PONDR) (*39*) are predicted for short structural elements that coincide with the location of MBI and MBII (Figure 1B). The MBI helix is amphipathic (Figure 1C) with polyproline (PP) stretches and regulatory phosphorylation sites flanking the sequence (*40*, *41*). The predicted helices, consisting of only seven residues each, may be present but only transiently.

B-Myc Association. The association of B-Myc with MM-1 and TBP is apparent from changes in the ^{15}N HSQC spectrum of B-Myc. Addition of either MM-1 (Figure 2B, red) or TBP (Figure 2C, cyan) differentially affects the HSQC spectrum by altering the frequency or intensity of certain peaks observed for free B-Myc. In addition, new peaks are apparent

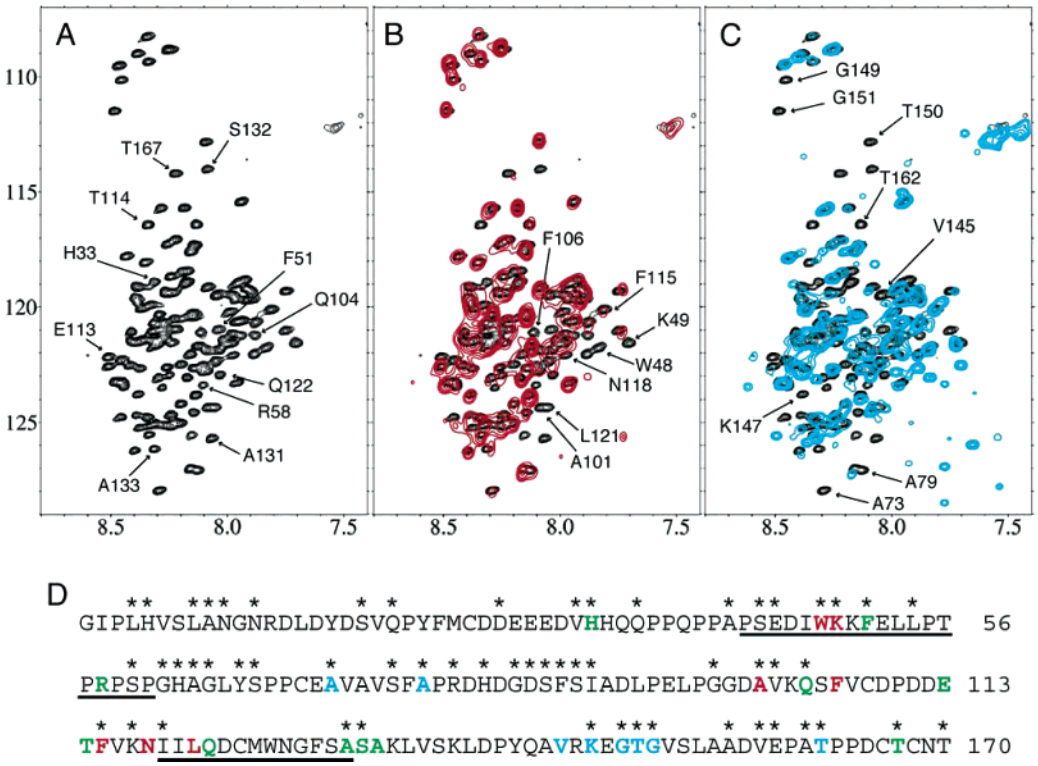

FIGURE 2: ^{15}N HSQC spectra of (A) B-Myc and (B) B-Myc with MM-1 (red) or (C) B-Myc with TBP overlaid with that of B-Myc alone (black). Labels indicate assigned free B-Myc peaks that show perturbations upon association with either MM-1 (panel B labels), TBP (panel C labels), or both (panel A labels). For the purpose of clarity, the data are plotted with the minimum contour threshold set higher than the intensity of perturbed peaks with reduced intensity in the presence of MM-1 or TBP (see the text for details). (D) Resonances with reduced intensity or altered frequency in the presence of MM-1 (red), TBP (cyan), or both (green) are mapped onto the sequence of B-Myc. Resonances for which relaxation rates were determined are marked with an asterisk. MBI and MBII are underlined.

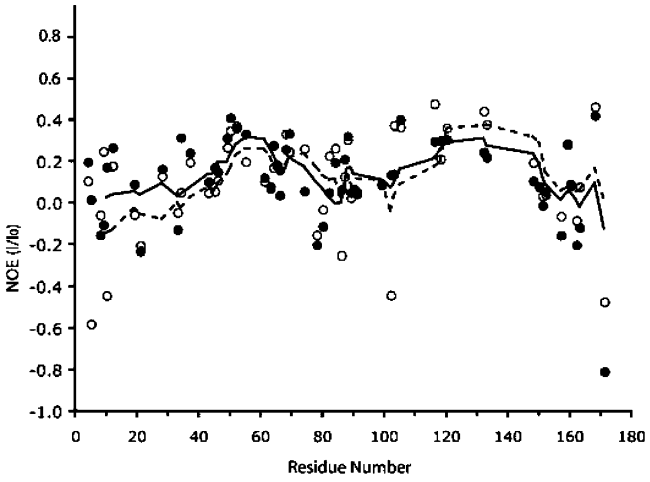

FIGURE 3: Individual values (circles) and moving average (five-residue window) (curves) of ^{1}H−^{15}N NOEs. Free B-Myc values are shown as a solid line with filled circles, and B-Myc−MM-1 values are shown as a dashed line and empty circles.

outside the region of the shifts for free B-Myc, particularly in the case of TBP. Nonetheless, a large increase in the extent of dispersion expected for formation of tertiary structure (*42*) was observed with neither MM-1 nor TBP.

We used CD spectropolarimetry to assess potential changes in the secondary structure of B-Myc upon binding of MM-1. Neither α-helical nor *β*-strand secondary structure is apparent in the free B-Myc spectrum (Figure 4A, black), which resembles that of a random coil protein. The CD spectrum of the GST−MM-1 fusion construct (Figure 4A, gray) exhibits the α-helical content expected for GST. The spectrum of B-Myc in the presence of the GST−MM-1 fusion construct and that calculated by summation of the free B-Myc and GST−MM-1 spectra are shown in Figure 4B. The calculated spectrum (gray) approximates that observed for the mixture of B-Myc and the GST−MM-1 fusion construct (black). From these results, we conclude that association with MM-1 induces neither secondary nor tertiary structure in B-Myc. Together, the limited change in chemical shift dispersion and the absence of an effect on the CD spectrum indicate that B-Myc interacts in a largely extended form, similar to that observed for the interaction of c-Myc with the SH3 domain of Bin-1 (*29*).

To further characterize intermolecular association of B-Myc, the specific residues affected by addition of the transactivation proteins were identified from the changes in the ^{15}N HSQC spectrum of B-Myc (*43*, *44*). Comparison of the HSQC spectra of B-Myc in the presence of MM-1 (Figure 2B, red) and TBP (Figure 2C, cyan) indicates that the perturbation to the HSQC spectrum depends on the transactivation protein and is likely the result of intermolecular association rather than nonspecific effects, such as crowding at high protein concentrations. A peak was considered to exhibit a perturbation relative to the free state if in the presence of MM-1 or TBP the peak was observed to shift >0.05 or 0.1 ppm in the ^{1}H or ^{15}N dimension, respectively. Additionally, a perturbation was considered to occur if the peak height was reduced to less than 40% of the intensity observed with free B-Myc. A high contour level is used to plot the overlaid spectra shown in Figure 2 so that peaks with reduced intensity in the presence of MM-1 or TBP do not appear in the plot.

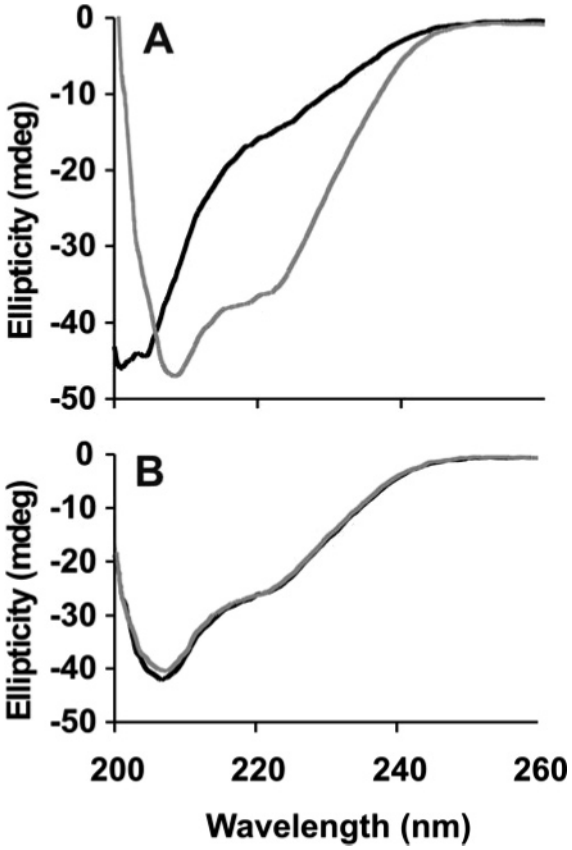

FIGURE 4: (A) CD spectra of B-Myc alone (black) and the GST−MM-1 fusion construct alone (gray). (B) CD spectrum for the B-Myc/GST−MM-1 solution calculated from the summation of spectra in panel A (black) and observed (gray).

Perturbations are observed for alternative resonances with MM-1 (labeled in Figure 2B) and TBP (labeled in Figure 2C), while some resonances are altered by both transactivation proteins (labeled in Figure 2A). The residues with HN resonances altered upon binding are also indicated in Figure 2D where residues affected by MM-1 are colored red, by TBP cyan, and by both MM-1 and TBP green. The spectral changes observed upon binding therefore distinguish these two transactivation proteins in terms of their binding. These HSQC perturbation results are consistent with previous deletion studies that show c-Myc residues 104−166 and 75−204 are required for binding to MM-1 and TBP, respectively (*24*, *25*), but the residue-specific information provided by NMR reveals distinct sites affected by binding MM-1 or TBP.[2] MM-1 association is mostly localized to MBI and MBII, whereas TBP perturbs residues in MBI and MBII and several residues C-terminal to MBII. As such, NMR identifies a previously unrecognized region affected by association of B-Myc with MM-1; resonances of several residues in MBI are perturbed by MM-1, which implies that MM-1 association involves both MBI and MBII.

Localization of MM-1 Interaction to MBI and MBII. The association of B-Myc and MM-1 was further characterized by heteronuclear relaxation. Given the clear distinction in the changes in the B-Myc HSQC spectrum upon addition of MM-1 and TBP, the effects on heteronuclear relaxation upon addition of MM-1 are reasonably assumed to be the result of intermolecular association. Changes in NMR dipolar relaxation rates for longitudinal (R_1), transverse (R_2), and nuclear Overhauser effect (NOE) relaxation reflect changes in effective molecular weight and rotational correlation time, τ_c, associated with intermolecular binding. In addition, R_2 is sensitive to a residue existing in more than one magnetic environment, such as free and bound states, and the rate of exchange between multiple environments.

^{15}N relaxation of main chain amide resonances was assessed for B-Myc alone and in the presence of MM-1. R_1 and R_2 were estimated for 57 resolved ^{15}N HSQC peaks from residues along the full length of B-Myc (Table 1). Association of B-Myc with MM-1 is apparent from effects on both R_1 and R_2. R_1 values increase approximately 12−43%, while R_2 values show substantially larger increases of 90 to >400%. The dependence of R_1 on τ_c passes through a maximum as τ_c increases, while R_2 increases continuously with τ_c. The trends in the changes in R_1 and R_2 between free B-Myc and B-Myc associated with MM-1 indicate that τ_c for B-Myc is near the value at the maximum R_1.

The site of intermolecular interaction was localized by monitoring changes in the R_2/R_1 ratio of individual residues. In the absence of chemical exchange, the R_2/R_1 ratio depends on a residue's τ_c value associated with molecular rotation on a nanosecond time scale and is less sensitive to faster local motions on a picosecond time scale (*45*, *46*). We use the R_2/R_1 ratio to assess the nature of the intermolecular association of B-Myc with MM-1 even though exchange cannot be ruled out and estimate an *apparent* correlation time, τ_c^{app}, by residue. In the case where exchange does contribute to R_2, τ_c^{app} reflects that exchange rather than an accurate rotational correlation time. Nonetheless, examination of changes in B-Myc τ_c^{app} values in the presence of MM-1 provides a convenient measure to contrast the effect of MM-1 association on individual residues of B-Myc.

Interaction with MM-1 differentially affects the R_2/R_1 ratio for individual residues of B-Myc (Figure 5). The results show that certain regions of B-Myc are strongly affected by association with MM-1 while others are not. A 3−5-fold increase in R_2/R_1 is localized to the regions surrounding MBI and MBII with some effect observed at the unique C-terminal region of B-Myc. Other regions show substantially smaller effects. The estimated τ_c^{app} values for MBI and MBII upon binding MM-1 increase by 3.3 and 5.0 ns, respectively, compared to those of regions outside the Myc homology boxes where τ_c^{app} increases an average of only 1.3 ns (Table 1). The τ_c^{app} values increase in the presence of MM-1 but remain significantly lower than values expected for a folded 36 kDa B-Myc−MM-1 complex. For example, the values of 6−9 ns in Table 1 for τ_c^{app} approximate the 8.3 and 9.0 ns values reported for ~13 kDa, globular proteins (*47*). B-Myc associated with MM-1, therefore, does not form a well-ordered globular dimer.

Figure 5 identifies B-Myc residues that associate strongly with MM-1. Of particular interest is the fact that the elevated R_2/R_1 values extend ~15 residues N-terminal to MBII starting from residue 102. This "extended" MBII form with residues 102−132, called here MBII*, is highly conserved between B-Myc and c-Myc, but the sequences of these two members of the Myc family have less conservation with N-, S-, and

[2] A small number of resonances that are not mapped to residues in Figure 2C, because overlap precluded a unique assignment of the resonance, were perturbed by binding.

Table 1: R_1 and R_2 Values for B-Myc and the B-Myc−MM-1 Complex[a]

	⟨R_1⟩ (s^{-1})			⟨R_2⟩ (s^{-1})			τ_c^{app} (ns)			⟨NOE⟩ (I/I_0)	
residues	B-Myc	B-Myc−MM-1	%Δ	B-Myc	B-Myc−MM-1	%Δ	B-Myc	B-Myc−MM-1	$\Delta\tau_c^{app}$ (ns)	B-Myc	B-Myc−MM-1
4−37	1.4	1.6	14.2	4.0	8.3	108	4.30	5.90	1.60	0.09	−0.01
43−57	**1.7**	**1.9**	**11.8**	**7.6**	**25.0**	**229**	**4.76**	**8.03**	**3.27**	**0.36**	**0.33**
61−102	1.4	1.9	35.7	4.4	8.5	88.9	4.51	5.79	1.28	0.12	0.10
103−133	**1.4**	**2.0**	**42.9**	**4.3**	**22.5**	**423**	**4.40**	**9.35**	**4.95**	**0.27**	**0.37**
148−171	1.3	1.6	23.1	3.5	7.2	106	3.75	4.76	1.01	−0.06	0.06

[a] Data for MBI and MBII* are bold. The apparent correlation time, τ_c^{app} (see the text), is calculated from the R_2/R_1 ratio by Tensor (*72*). The percent change is represented as (bound − free)/free.

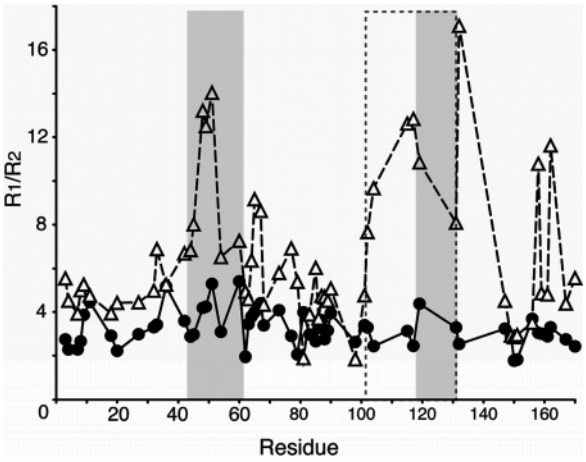

FIGURE 5: R_2/R_1 ratios measured at a field strength of 750 MHz for B-Myc (●) and the B-Myc−MM-1 complex (△). MBI and MBII are shaded. MBII* includes the 15 N-terminal residues and is shown in a dotted box.

L-Myc. The observation by NMR relaxation suggests that MM-I may bind preferentially, or perhaps more stably, to c-Myc and B-Myc (*3*, *48*, *49*). We conclude that B-Myc interacts with MM-1 through both MBI and MBII but preferentially through an expanded MBII motif. An intact MBII was shown previously to be essential for c-Myc and MM-1 interaction in mammalian two-hybrid assays (*24*). A large increase in the R_2/R_1 ratio for residues 159 and 163 in the unique C-terminal tail also suggests that the binding of MM-1 may impact this region of B-Myc as well.

Our results show that MBI, MBII, and possibly the unique C-terminal tail are involved in the association of MM-1 with B-Myc, although the precise nature of the interaction in terms of structure and residues in direct contact as well as the impact on the function of either protein in vivo remains to be determined.

CONCLUSIONS

NMR spectroscopy was used to characterize the structural order of B-Myc both free and bound to transactivation inhibitor MM-1 and transactivation activator TBP. Free B-Myc is unfolded and flexible over its 171-residue length. Relaxation properties are consistent with a more collapsed but disordered state characteristic of molten globules, with residues forming MBI and MBII showing a slight tendency toward slower mobility. An understanding of the functional advantage of intrinsically disordered proteins (*50*−*52*) based largely on the residue-level structural information provided by NMR spectroscopy (*53*) is starting to emerge. Intrinsically disordered regions of certain proteins are known to adopt ordered structure upon binding (*54*−*58*). It has been suggested that linking protein−protein association to folding allows for a specific interaction with low affinity (*59*) that is be important for reversible binding of regulatory proteins, including transcription factors.

An important finding determined from the residue-level information of NMR in this study is that the associations of MM-1 and TBP with B-Myc are distinct. Further, NMR relaxation data of B-Myc with MM-1 clearly show that intermolecular association is localized to specific residues in the more collapsed regions of MBI and MBII, but we find no compelling evidence from CD, chemical shift dispersion, or homonuclear NOEs that binding to MM-1 induces secondary or tertiary structure.

That binding is specific, yet substantial regions remain unfolded in the B-Myc−MM-1 complex, appears to differ somewhat from that in certain other intrinsically disordered protein complexes in which more ordered, folded states are acquired upon binding (*53*). The binding characteristics of the B-Myc−MM-1 complex are more consistent with the recent description of the interaction of c-Myc with the Bin-1 SH3 domain (*29*). In contrast to association of Myc with Bin-1, however, association of Myc with MM-1 does not occur via a recognized binding domain, such as an SH2 or SH3 domain, as MM-1 has no such domains as determined by sequence analysis. Specific binding of Myc to one transactivation domain, while much of Myc remains unfolded, provides a mechanism for the requirement that Myc functions by specifically recognizing numerous binding partners, some simultaneously. Regions remaining unfolded in one association complex can provide the specificity determinants for recognition of another binding partner.

The diverse cellular functions of the Myc protein family depend on the N-terminal domain of the protein where many protein−protein interactions are mediated by MBI and MBII (*6*, *8*). HSQC perturbation shows the interactions of B-Myc with MM-1, a transactivation inhibitor, to be distinct from those with TBP, a transactivation activator. MM-1 binding affects both MBI and MBII, but association of TBP with Myc influences mostly MBII and sequences C-terminal to this core motif. Exploiting NMR relaxation to more fully characterize Myc protein−protein associations and the influence of Myc point mutations, such as those that replace c-Myc Trp 135 (corresponding to B-Myc Trp 126), which is important for transformation (*60*, *61*), yet dispensable for transactivation (*28*, *60*), will be of interest.

Our results find that the effect on MBII of the interaction between B-Myc and MM-I extends approximately 15 residues N-terminal to MBII. The extended region, MBII*, is noteworthy in light of the sequence similarity between

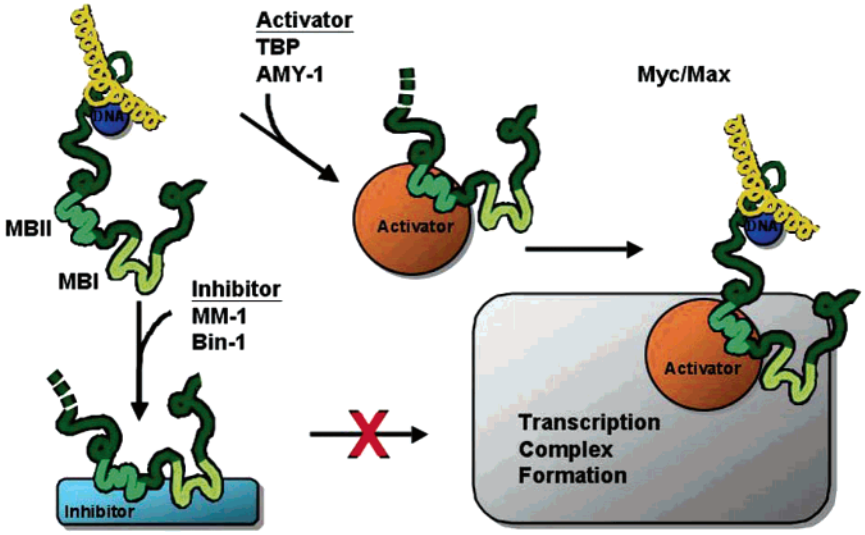

FIGURE 6: Model of possible activation and/or inactivation of transactivation by B-Myc and the N-terminal region of c-Myc proteins. Transcription activation is by association of activators such as TBP with MBII and further assembly with other factors that recognize regions near MBI. In contrast, binding by repressors, such as MM-1, extends across MBI and MBII* and prevents formation of the transcription complex.

B-Myc and c-Myc. While MBI and MBII are conserved across all members of the Myc family, only B-Myc and c-Myc share extensive sequence similarity for residues N-terminal to MBII (Figure 2A). The higher degree of similarity between B-Myc and c-Myc is apparent from the observation that B-Myc inhibits c-Myc activity presumably by competing for c-Myc N-terminal interacting proteins (*5*). Our data are the first to suggest that the Myc proteins utilize amino acids outside of the highly conserved MBI and MBII to control the affinity and/or stability of interactions with other proteins. This trait also holds for the interaction of B-Myc with TBP, which extends to residues C-terminal to MBII and more highly conserved between B-Myc and c-Myc than other Myc family members.

In addition to the interaction of MM-I with amino acids N-terminal to MBII, we report a previously undetected interaction between MM-I and MBI. MBI sits in a structurally intriguing region that is predicted to form a short amphipathic helix (Figure 1B) positioned between two polyproline stretches. MBI is located just N-terminal to two known regulatory phosphorylation sites that play a major role in controlling the overall activity of Myc by triggering protein turnover (*40*, *62*−*67*). Given the involvement of MBI in MM-1 association, phosphorylation may also be important in modulating Myc protein−protein interactions by allowing the N-terminal domain to adopt a structure that differentially affects binding of activators and inhibitors.

From the data reported here, we propose a model for Myc regulation in which MBI and MBII bind differentially to alternative regulatory partners (Figure 6). Transcriptional activation involves association of Myc with activators such as TBP and Amy-I (*68*) mediated through MBII. Further assembly with additional transcription complex factors could require access to regions of Myc near MBI. On the other hand, transcriptional repressor MM-1 associates with an interface of B-Myc extending to both MBI and MBII and thus could inhibit proper association of other protein factors of the transcription complex required for transcription. The extended interfaces that have been described for the interaction of Myc with transcriptional repressors such as MM-I (current study and ref *24*), Bin1 (*69*), and p107 (*70*) suggest that these proteins may serve as a type of "molecular sponge" that interacts with MBII and now MBI to preclude the formation of a productive multiprotein complex needed to activate transcription. Growth signals that culminate in the partial, or complete, release of the transcriptional repressors allow key activators to bind to Myc and recruit the remaining components of the transcriptional machinery.

REFERENCES

1. Ingvarsson, S., Asker, C., Axelson, H., Klein, G., and Sumegi, J. (1988) Structure and expression of B-myc, a new member of the myc gene family, *Mol. Cell. Biol. 8*, 3168−74.
2. Gregory, M. A., Xiao, Q., Cornwall, G. A., Lutterbach, B., and Hann, S. R. (2000) B-Myc is preferentially expressed in hormonally-controlled tissues and inhibits cellular proliferation, *Oncogene 19*, 4886−95.
3. Asker, C. E., Magnusson, K. P., Piccoli, S. P., Adersson, K., Klein, G., Cole, M. D., and Wiman, K. G. (1995) Mouse and rat B-Myc share amino acid sequence homology with the c-Myc transcriptional activator domain and contain a B-Myc specific carboxy terminal region, *Oncogene 11*, 1963−9.
4. Cornwall, G. A., Collis, R., Xiao, Q., Hsia, N., and Hann, S. R. (2001) B-Myc, a proximal caput epididymal protein, is dependent on androgens and testicular factors for expression, *Biol. Reprod. 64*, 1600−7.
5. Resar, L. M. S., Dolde, C., Barrett, J. F., and Dang, C. V. (1993) B-Myc Inhibits Neoplastic Transformation and Transcriptional Activation by c-Myc, *Mol. Cell. Biol. 13*, 1130−6.
6. Henriksson, M., and Luscher, B. (1996) Proteins of the Myc network: Essential regulators of cell growth and differentiation, *Adv. Cancer Res. 68*, 109−82.
7. Nesbit, C. E., Tersak, J. M., and Prochownik, E. V. (1999) MYC oncogenes and human neoplastic disease, *Oncogene 18*, 3004−16.
8. Oster, S. K., Ho, C. S., Soucie, E. L., and Penn, L. Z. (2002) The myc oncogene: MarvelouslY Complex, *Adv. Cancer Res. 84*, 81−154.
9. Felsher, D. W., and Bradon, N. (2003) Pharmacological inactivation of MYC for the treatment of cancer, *Drug News Perspect. 16*, 370−4.
10. Hermeking, H. (2003) The MYC oncogene as a cancer drug target, *Curr. Cancer Drug Targets 3*, 163−75.
11. Prochownik, E. V. (2004) c-Myc as a therapeutic target in cancer, *Expert Rev. Anticancer Ther. 4*, 289−302.
12. Thompson, E. B. (1998) The many roles of c-Myc in apoptosis, *Annu. Rev. Physiol. 60*, 575−600.

13. Dang, C. V. (1999) c-Myc target genes involved in cell growth, apoptosis, and metabolism, *Mol. Cell. Biol. 19*, 1−11.
14. Peters, M. A., and Taparowsky, E. J. (1998) Target genes and cellular regulators of the Myc transcription complex, *Crit. Rev. Eukaryotic Gene Expression 8*, 277−96.
15. Patel, J. H., Loboda, A. P., Showe, M. K., Showe, L. C., and McMahon, S. B. (2004) Analysis of genomic targets reveals complex functions of MYC, *Nat. Rev. Cancer 4*, 562−8.
16. Prendergast, G. (1999) Mechanisms of apoptosis by c-Myc, *Oncogene 18*, 2967−87.
17. Grandori, C., and Eisenman, R. N. (1997) Myc target genes, *Trends Biochem. Sci. 22*, 177−81.
18. Oster, S. K., Mao, D. Y., Kennedy, J., and Penn, L. Z. (2003) Functional analysis of the N-terminal domain of the Myc oncoprotein, *Oncogene 22*, 1998−2010.
19. Kato, G. J., Barrett, J., Villa-Garcia, M., and Dang, C. V. (1990) An amino-terminal c-Myc domain required for neoplastic transformation activates transcription, *Mol. Cell. Biol. 10*, 5914−20.
20. Blackwood, E. M., and Eisenman, R. N. (1991) Max: A helix-loop-helix zipper protein that forms a sequence-specific DNA-binding complex with Myc, *Science 251*, 1211−7.
21. Ayer, D. E., Kretzner, L., and Eisenman, R. N. (1993) Mad: A heterodimeric partner for max that antagonizes Myc transcriptional activity, *Cell 72*, 211−22.
22. Nair, S. K., and Burley, S. K. (2003) X-ray structures of Myc-Max and Mad-Max recognizing DNA: Molecular bases for regulation by proto-oncogenic transcription factor, *Cell 112*, 193−205.
23. Sakamuro, D., and Prendergast, G. (1999) New myc-interacting proteins: A second myc network emerges, *Oncogene 18*, 2942−54.
24. Mori, K., Maeda, Y., Kitaura, H., Taira, T., Iguchi-Ariga, S. M. M., and Ariga, H. (1998) MM-1, a novel c-Myc-associating protein that represses transcriptional activity of c-Myc, *J. Biol. Chem. 273*, 29794−800.
25. Hateboer, G., Timmers, H. T. M., Rustgi, A. K., Billaud, M., van'T Veer, L. J., and Bernards, R. (1993) TATA-binding protein and the retinoblastoma gene product bind to overlapping epitopes on c-Myc and adenovirus EIA protein, *Proc. Natl. Acad. Sci. U.S.A. 90*, 8489−93.
26. Maheswaran, S., Lee, H. Y., and Sonenshein, G. E. (1994) Intracellular association of the protein product of the c-Myc oncogene with the TATA-binding protein, *Mol. Cell. Biol. 14*, 1147−52.
27. McEwan, I. J., Dahlman-Wright, K., Ford, J., and Wright, A. P. H. (1996) Functional interaction of the c-Myc transactivation domain with the TATA binding protein: Evidence for an induced fit model of transactivation domain folding, *Biochemistry 35*, 9584−93.
28. Barrett, J. F., Lee, L. A., and Dang, C. V. (2005) Stimulation of Myc transactivation by the TATA binding protein in promoter-reporter assays, *BMC Biochem. 6*, doi 10.1186/1471-2091-6-7.
29. Pineda-Lucena, A., Ho, C. S. W., Mao, D. Y. L., Sheng, Y., Laister, R. C., Muhandiram, R., Lu, Y., Seet, B. T., Katz, S., Szyperski, T., Penn, L. Z., and Arrowsmith, C. H. (2005) A structure-based model of the c-Myc/Bin1 protein interaction shows alternative splicing of Bin1 and c-Myc phosphorylation are key binding determinants, *J. Mol. Biol. 351*, 182−94.
30. Farrow, N. A., Muhandiram, R., Singer, A. U., Pascal, S. M., Kay, C. M., Gish, G., Shoelson, S. E., Pawson, T., Forman-Kay, J. D., and Kay, L. E. (1994) Backbone dynamics of a free and a phosphopeptide-complexed Src homology 2 domain studied by ^{15}N NMR relaxation, *Biochemistry 33*, 5984−6003.
31. Goddard, T. G., and Kneller, D. G. (2002) *Sparky 3*, University of California, San Francisco.
32. Schwarzinger, S., Kroon, G. J. A., Foss, T. R., Wright, P. E., and Dyson, H. J. (2000) Random coil chemical shifts in acidic 8 M urea: Implementation of random coil shift data in NMRView, *J. Biomol. NMR 18*, 43−8.
33. Schwarzinger, S., Kroon, G. J. A., Foss, T. R., Chung, J., Wright, P. E., and Dyson, H. J. (2001) Sequence-Dependent Correction of Random Coil NMR Chemical Shifts, *J. Am. Chem. Soc. 123*, 2970−8.
34. Wishart, D. S., and Sykes, B. D. (1994) The ^{13}C chemical-shift index: A simple method for identification of protein secondary structure using ^{13}C chemical-shift data, *J. Biomol. NMR 4*, 171−80.
35. Farrow, N. A., Zhang, O., Muhandiram, R., Forman-Kay, J. D., and Kay, L. E. (1997) Characterization of the backbone dynamics of folded and denatured states of an SH3 domain, *Biochemistry 36*, 2390−402.
36. Schwalbe, H., Fiebig, K. M., Buck, M., Jones, J. A., Grimshaw, S. B., Spencer, A., Glaser, S. J., Smith, L. J., and Dobson, C. M. (1997) Structural and dynamical properties of a denatured protein. Heteronuclear 3D NMR experiments and theoretical simulations of lysozyme in 8 M urea, *Biochemistry 36*, 8977−91.
37. Cavagnero, S., Nishimura, C., Schwarzinger, S., Dyson, H. J., and Wright, P. E. (2001) Conformational and dynamic characterization of the molten globule state of an apomyoglobin mutant with an altered folding pathway, *Biochemistry 40*, 14459−67.
38. Rost, B., and Sander, C. (1993) Prediction of protein secondary structure at better than 70% accuracy, *J. Mol. Biol. 232*, 584−99.
39. Iakoucheva, L. M., Brown, C. J., Lawson, J. D., Obradovic, Z., and Dunker, A. K. (2002) Intrinsic Disorder in Cell-signalling and Cancer-associated Proteins, *J. Mol. Biol. 323*, 573−84.
40. Gregory, M. A., and Hann, S. R. (2000) c-Myc proteolysis by the ubiquitin-proteosome pathway: Stabilization of c-Myc in Burkitt's Lymphoma cells, *Mol. Cell. Biol. 20*, 2423−35.
41. Henriksson, M., Bakardjiev, A., Klein, G., and Luscher, B. (1993) Phosphorylation site mapping in the N-terminal domain of c-Myc modulates transforming potential, *Oncogene 8*, 3199−209.
42. Dyson, H. J., and Wright, P. E. (2004) Unfolded proteins and protein folding studied by NMR, *Chem. Rev. 104*, 3607−22.
43. Otting, G. (1993) Experimental NMR techniques for studies of protein−ligand interactions, *Curr. Opin. Struct. Biol. 3*, 760−8.
44. Gao, G. H., Williams, J. G., and Campbell, S. L. (2004) Protein−protein interaction analysis by nuclear magnetic resonance spectroscopy, *Methods Mol. Biol. 261*, 79−92.
45. Clore, G. M., Driscoll, P. C., Wingfield, P. T., and Gronenborn, A. M. (1990) Analysis of the backbone dynamics of Interleukin-1β using two-dimensional inverse detected heteronuclear ^{15}N-^{1}H NMR spectroscopy, *Biochemistry 29*, 7387−401.
46. Kay, L. E., Torchia, D. A., and Bax, A. (1989) Backbone dynamics of proteins as studied by N-15 inverse detected heteronuclear NMR spectroscopy: Application to staphylococcal nuclease, *Biochemistry 28*, 8972−9.
47. de la Torre, J. G., Huertas, M. L., and Carrasco, B. (2000) HYDRONMR: Prediction of NMR relaxation of globular proteins from atomic-level structures and hydrodynamic calculations, *J. Magn. Reson. 147*, 138−46.
48. Colby, W. W., Chen, E. Y., Smith, D. H., and Levinson, A. D. (1983) Identification and nucleotide sequence of a human locus homologous to the v-myc oncogene of avian myelocytomatosis virus MC29, *Nature 301*, 722−5.
49. Flinn, E. M., Bush, C. M. C., and Wright, A. P. H. (1998) Myc boxes, which are conserved in myc family proteins, are signals for protein degradation via the proteasome, *Mol. Cell. Biol. 18*, 5961−9.
50. Uversky, V. N., Gillespie, J. R., and Fink, A. L. (2000) Why are "natively unfolded" proteins unstructured under physiologic conditions? *Proteins: Struct., Funct., Genet. 41*, 415−27.
51. Uversky, V. N. (2002) Natively unfolded proteins: A point where biology waits for physics, *Protein Sci. 11*, 739−56.
52. Tompa, P. (2002) Intrinsically unstructured proteins, *Trends Biochem. Sci. 27*, 527−33.
53. Dyson, H. J., and Wright, P. E. (2005) Intrinsically unstructured proteins and their functions, *Nat. Rev. Mol. Cell Biol. 6*, 197−208.
54. Fletcher, C. M., and Wagner, G. (1998) The interaction of eIF4E with 4E-BP1 is an induced fit to a completely disordered protein, *Protein Sci. 7*, 1639−42.
55. Fletcher, C. M., McGuire, A. M., Gingras, A. C., Li, H. J., Matsuo, H., Sonenberg, N., and Wagner, G. (1998) 4E binding proteins inhibit the translation factor eIF4E without folded structure, *Biochemistry 37*, 9−15.
56. Kumar, R., Volk, D. E., Li, J. Q., Lee, J. C., Gorenstein, D. G., and Thompson, E. B. (2004) TATA box binding protein induces structure in the recombinant glucocorticoid receptor AF1 domain, *Proc. Natl. Acad. Sci. U.S.A. 101*, 16425−30.
57. Zhou, P., Lugovskoy, A. A., McCarty, J. S., Li, P., and Wagner, G. (2001) Solution structure of DFF40 and DFF45 N-terminal domain complex and mutual chaperone activity of DFF40 and DFF45, *Proc. Natl. Acad. Sci. U.S.A. 98*, 6051−5.
58. Radhakrishnan, I., PerezAlvarado, G. C., Parker, D., Dyson, H. J., Montminy, M. R., and Wright, P. E. (1997) Solution structure of the KIX domain of CBP bound to the transactivation domain of CREB: A model for activator:coactivator interactions, *Cell 91*, 741−52.

59. Schultz, G. E. (1979) Nucleotide Binding Proteins, in *Molecular Mechanisms of Biological Recognition* (Balaban, M., Ed.) pp 79−94, Elsevier/North-Holland Biomedical Press, New York.
60. Brough, D., Hofmann, T., Ellwood, K., Townley, R., and Cole, M. (1995) An essential domain of the c-myc protein interacts with a nuclear factor that is also required for E1A-mediated transformation, *Mol. Cell. Biol. 15*, 1536−44.
61. Prescott, J. E., Osthus, R. C., Lee, L. A., Lewis, B. C., Shim, H., Barrett, J. F., Guo, Q. B., Hawkins, A. L., Griffin, C. A., and Dang, C. V. (2001) A novel c-Myc-responsive gene, JPO1, participates in neoplastic transformation, *J. Biol. Chem. 276*, 48276−84.
62. Bahram, F., vonderLehr, N., Cetinkaya, C., and Larsson, L.-G. (2000) c-Myc hot spot mutations in lymphomas result in inefficient ubiquitination and decreased proteasome-mediated turnover, *Blood 95*, 2104−10.
63. Niklinski, J., Claassen, G., Meyers, C., Gregory, M. A., Allegra, C. J., Kaye, F. J., Hann, S. R., and Zajac-Kaye, M. (2000) Disruption of Myc-tubulin interaction by hyperphosphorylation of c-Myc during mitosis or by constitutive hyperphosphorylation of mutant c-Myc in Burkitt's lymphoma, *Mol. Cell. Biol. 20*, 5276−84.
64. Salghetti, S. E., Kim, S. Y., and Tansey, W. P. (1999) Destruction of Myc by ubiquitin-mediated proteolysis: Cancer-associated and transforming mutations stabilize Myc, *EMBO J. 18*, 717−26.
65. Sears, J. R., Ohtani, K., and Nevins, J. (2000) Identification of positively and negatively acting elements regulating expression of the E2F2 gene in response to cell growth signals, *Mol. Cell. Biol. 17*, 5227−35.
66. Dominguez-Sola, D., and Dalla-Favera, R. (2004) PINning down the c-Myc oncoprotein, *Nat. Cell Biol. 6*, 288−9.
67. Yeh, E., Cunningham, M., Arnold, H., Chasse, D., Monteith, T., Ivaldi, G., Hahn, W. C., Stukenberg, P. T., Shenolikar, S., Uchida, T., Counter, C. M., Nevins, J. R., Means, A. R., and Sears, R. (2004) A signalling pathway controlling c-Myc degradation that impacts oncogenic transformation of human cells, *Nat. Cell Biol. 6*, 308−18.
68. Taira, T., Maeda, J., Onishi, T., Kitaura, H., Yoshida, S., Kato, H., Ikeda, M., Tamai, K., Iguchi-Ariga, S. M. M., and Ariga, H. (1998) AMY-1, a novel C-MYC binding protein that stimulates transcription activity of C-MYC, *Genes Cells 3*, 549−65.
69. Sakamuro, D., Elliot, K. J., Wechsler-Reya, R., and Prendergast, G. (1996) BIN1 is a novel MYC-interacting protein with features of a tumor suppressor, *Nat. Genet. 14*, 69−77.
70. Hoang, A. T., Lutterbach, B., Lewis, B. C., Yano, T., Chou, T.-Y., Barrett, J. F., Raffeld, M., Hann, S. R., and Dang, C. V. (1995) A link between increased transforming activity of lymphoma-derived MYC mutant alleles, their defective regulation by p107, and altered phosphorylation of the c-Myc transactivation domain, *Mol. Cell. Biol. 15*, 4031−42.
71. Thompson, J. D., Higgins, D. G., and Gibson, T. J. (1994) CLUSTAL W: Improving the sensitivity of progressive multiple sequence alignment through sequence weighting, position-specific gap penalties and weight matrix choice, *Nucleic Acids Res. 22*, 4673−80.
72. Dosset, P., Hus, J.-C., Blackledge, M., and Marion, D. (2000) Efficient analysis of macromolecular rotational diffusion from heteronuclear relaxation data, *J. Biomol. NMR 16*, 23−8.

BI060379N